Radio-Frequency Field Measurement Using Thin Artificial Magnetic Conductor Absorber

Satoshi Yagitani [#1], Tomohiro Sunahara [#], Tatsuya Nakagawa [#], Daisuke Hiraki [#], Yoshiyuki Yoshimura [*], Hirokazu Sugiura [*]

[#] *Graduate School of Natural Science and Technology, Kanazawa University*
Kakuma-machi, Kanazawa 920-1192, Japan

[1] yagitani@is.t.kanazawa-u.ac.jp

[*] *Industrial Research Institute of Ishikawa*
2-1 Kuratsuki, Kanazawa 920-8203, Japan

***Abstract*—The thin radio-frequency (RF) absorber constructed with an artificial magnetic conductor (AMC) surface is used as a sensor array to measure incident 2-d RF field (amplitude and phase) distributions. The AMC surface employs a 2-d dense array of mushroom-type square metal patches on a dielectric substrate. Incident waves are absorbed by the lumped resistors interconnecting the metal patches on the surface, when they are matched with the incident wave impedance at the resonance frequency of the mushroom structure. A 2-d distribution of the amplitude and phase of the incident RF field is obtained by directly measuring those of the voltages induced on the individual resistors. The validity of this new technique of RF field measurement is evaluated using electromagnetic simulation. It is confirmed that the voltage induced on the resistor can be used to monitor the incident (absorbed) RF electric field. For a finite-sized absorber the measurement accuracy is degraded near the outer edge due to edge reflections. This technique is expected to be useful for capturing the snapshots of RF field distributions in situ, while the electromagnetic environment is almost undisturbed by the AMC absorber.**

I. Introduction

Artificial magnetic conductors (AMC) realized with frequency-selective surfaces and metamaterial surfaces have been employed to design thin radio-frequency (RF) absorbers [1]-[3]. An incident wave is absorbed by the additional resistive component to the AMC surface which exhibits a high-impedance feature around its resonance frequency. As a new application of such an absorber, recently it was proposed that a kind of AMC absorber (tentatively termed an "electromagnetic band-gap (EBG) absorber") could be used for monitoring 2-d power distributions of an RF wave incident on the absorber surface [4]. Lumped resistors interconnecting the square patches on the mushroom-type (EBG) surface structure were used to absorb the incident RF power, which was monitored by a 2-d array of power detectors attached to the resistors. The power detection capability was validated by a preliminary experiment. With this technique the snapshots of RF power distributions could be captured and visualized in situ, while the electromagnetic environment is almost undisturbed by the AMC absorber.

In this study, as an extension of [4], we propose to make a measurement of the 2-d distribution of the incident wave fields (both amplitude and phase), by directly measuring the voltages induced on the individual lumped resistors. The relationship between the induced voltages and the incident electric fields is evaluated by means of electromagnetic simulation. In particular the effect of finite-sized absorber is examined. This technique is expected to be useful for capturing RF field distributions in situ, which should be crucial for identifying the direction-of-arrivals and source locations of the incoming waves.

II. Measurement Principle of RF Field by AMC Absorber

In [4], a thin absorber was designed employing a metasurface having an EBG structure; an array of 2-d mushroom-type unit cells with square metal patches were formed on a thin dielectric substrate to obtain an AMC feature. Absorption was achieved by the lumped resistors inserted between the adjacent patches. Fig. 1 (a) illustrates the configuration of the absorber. When the gap g between the adjacent patches is much smaller than the patch size w, and the cell periodicity $a = w + g$ is much smaller than the wavelength, the mushroom structure behaves as a parallel connection of the effective capacitance and inductance [5]. If the substrate is lossless the incident power is absorbed by the lumped resistors; the resistance R = 377 Ω (matched with the free-space wave impedance η_0 for the case of normal incidence) completely absorbs the incident wave power at the LC resonance frequency, as shown by an equivalent-circuit in Fig. 1 (b). The power absorbed by each resistor is dependent on the incident polarization; the amounts of RF power with its electric field polarized in the *x*- and *y*-directions are absorbed by the resistors connecting the adjacent patches in the *x*- and *y*-directions, respectively. In either case, the power absorbed by each resistor, P, should be equal to "the Poynting flux of the incident wave" times "the area of one unit cell," $P = E^2a^2/2\eta_0$, where E is the incident electric field. In [4], the amounts of power consumed by the individual resistors were measured by power detectors attached to them.

When the incident power is completely absorbed (consumed) by the surface resistors at the resonance frequency (when $R = \eta_0$), the voltage induced on each resistor becomes $V = (2PR)^{1/2} = Ea$, "the incident electric field" times "the unit cell size." In this case the phase of the electric field should be preserved as the phase of the voltage, unless any extra reactive component is introduced. Thus, by measuring the voltage induced on each resistor, we can expect that the amplitude and phase of the incident electric field can exactly be measured.

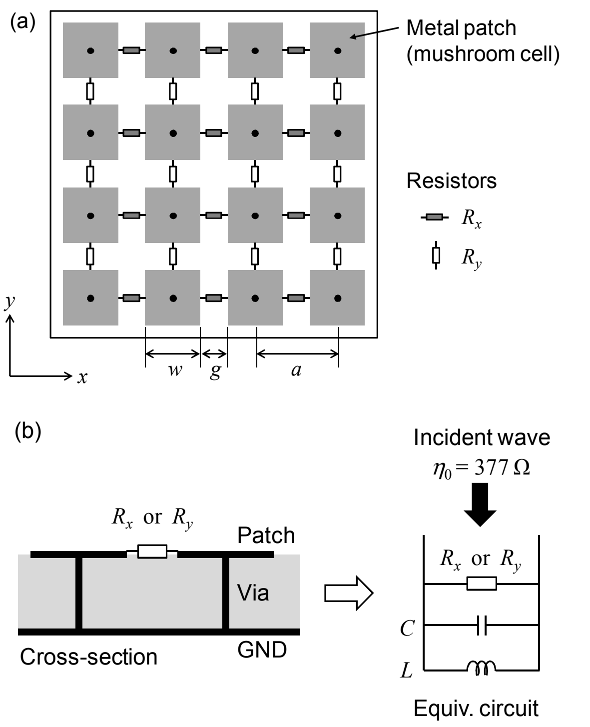

Fig. 1. The AMC absorber for RF field measurement: (a) surface structure, and (b) its cross section and equivalent circuit

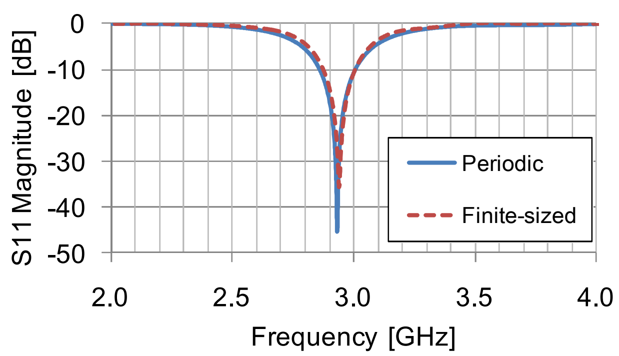

Fig. 2. Reflection characteristics of the AMC absorber for the normal incidence of a plane wave

III. Simulation

A. AMC Absorber Model

The geometrical and constitutional parameters of the thin AMC absorbers analyzed in this study by electromagnetic (EM) simulation were as follows. The size of a patch, the gap between the adjacent patches, and the cell periodicity were respectively w = 20 mm, g = 1 mm, and a = 21 mm. The thickness and dielectric constant of a loss-free substrate were 1.6 mm and 4.56. All the lumped resistors were set to be 377 Ω. Here we evaluated two simulation models. One was a periodic absorber: A square area containing a unit cell of the absorber was modeled by defining the periodic boundary condition, which corresponds to simulating infinitely extending periodic unit cells. A plane wave was incident on this model. The other was a finite-sized absorber: 15 by 15 cells were formed on 31.4 cm by 31.4 cm square substrate, which was illuminated by either a plane wave or a spherical wave. These EM simulations were performed with CST Microwave Studio commercial software.

B. Plane Wave Incidence

At first a plane wave with its electric field of 1.0 V/m polarized in the y-direction was incident vertically onto the periodic absorber. A solid blue line in Fig. 2 plots the reflection coefficient (S_{11}) of the absorber. At a resonance frequency of 2.928 GHz S_{11} = -45 dB was achieved. In this case the voltage induced on a lumped resistor mounted in the y-direction (R_y) was 0.021 V, which is exactly the value expected from the incident electric field intensity multiplied by the size of one unit cell (21 mm). It was also confirmed that the phase of the induced voltage was exactly the same as that of the incident electric field on the absorber surface. Thus both the amplitude and phase of the incident electric field are accurately retrieved from the voltage induced on the lumped resistor, when the incident plane wave is completely absorbed by the periodic absorber.

Next a plane wave with the same amplitude and polarization as above was incident onto the finite-sized absorber. The reflection coefficient was evaluated at the point 45 cm above the center of the absorber surface, as shown by a broken red line in Fig. 2. A little degraded reflection of -35 dB was obtained at a slightly different resonance frequency of 2.936 GHz. These were most likely caused by the undesired reflection at the edges of the absorber. (Note that the absorber size was about 3λ by 3λ at the resonance frequency.) Fig. 3 shows the 2-d distribution of the electric field (E_y) on the absorber surface at 2.93 GHz, where (a) and (b) are the amplitude and phase of the electric field, respectively, which were calculated from the voltage (V_y) induced on the lumped resistor mounted in the y-direction (R_y), as $E_y = V_y/a$. The E_y values at selected points are put on each color map divided into 15 by 14 areas in the x- and y-directions, which correspond to the locations of the 2-d array of R_y resistors (see Fig. 1 (a)). In Fig. 3 (a), the calculated (*i.e.*, measured) amplitude was obtained with the error less than 10% (less than 1 dB), except near the outer edges of the absorber where the incident plane wave was distorted by the edge reflection. The edge reflection also caused the appearance of an interference pattern on the surface. Fig. 3 (b) plots a snapshot of the phase distribution at the timing when the phase of the incident electric field became 0 on the absorber surface. This means that the figure corresponds to the measured phase error, which was within +/-10degrees, again except for the outer edge regions.

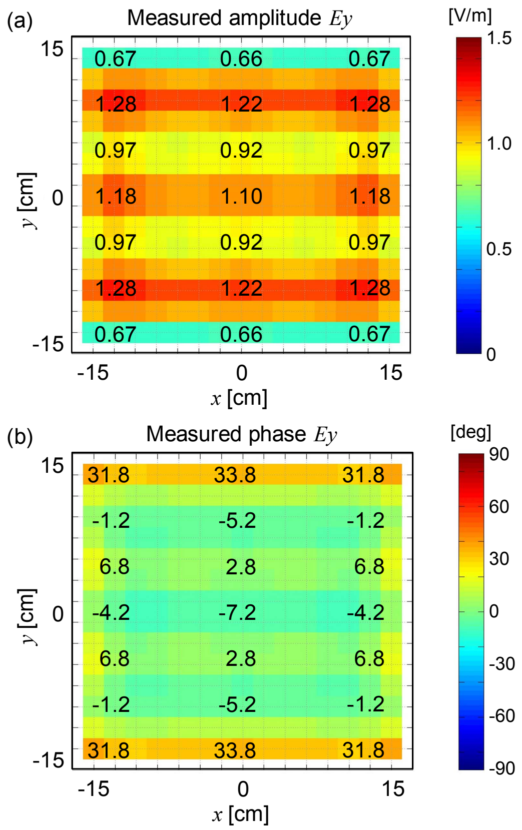

Fig. 3. Two-dimensional distributions of (a) amplitude and (b) phase of the plane-wave electric field measured on the absorber surface: the electric field was calculated from the voltages induced on the lumped resistors

C. Spherical Wave Incidence

The finite-sized absorber was illuminated by a spherical wave at 2.93 GHz radiated from a half-wavelength dipole. The center of the dipole was placed 15 cm above the center of the finite-sized absorber, and the dipole axis was along the y-direction. A power of 5 mW was radiated. Fig. 4 shows the amplitude and phase distributions of the E_y component of the electric field on the absorber surface. Fig. 4 (a) is the amplitude distribution of the incident electric field (E_{y0}), whereas (b) shows the calculated (measured) one (E_y) from the induced voltages. Here the numbers on the color map in Fig. 4 (b) represent the measurement error ($E_y(x,y)$ divided by $E_{y0}(x,y)$) at each point on the surface. The measured amplitude was almost consistent with the incident one, with an error about 10% in the inland area, which increased up to 30% toward the outer edges. As in the case of plane wave incidence, this error was caused by the interference due to the edge reflection. A snapshot of the phase distribution of the incident electric field is plotted in Fig. 4 (c), which is compared with the measured phase distribution in (d), where the numbers show the difference between the measured and incident phases. The measured phases were also consistent with the incident one, with an error of a few degrees up to several tens of degrees toward the edges. Fig. 5 shows the electric field vectors (E_x-E_y polarizations) on the absorber surface; the figures (a) and (b) plot the incident and measured vectors, respectively. The measured E_x and E_y were calculated from the voltages induced on R_x and R_y resistors. As in the case of amplitude and phase measurement, the vectors almost consistent with the incident ones were measured, with gradual distortion toward the outer edges.

It is noted that in this study the effect of the oblique incidence has not been considered. The AMC absorber exhibits different absorption (and reflection) performance at different angles of incidence [2][3]. As the voltages induced on the lumped resistors on the surface would be affected by the reflected electromagnetic fields in addition to the incident ones, it is necessary to evaluate the effect of oblique incidence for further validating the RF measurement technique proposed here.

IV. Conclusion

A technique to measure the 2-d RF field distribution using the AMC absorber was proposed and validated by simulation. On the basis of the voltages induced on the lumped resistors attached on the AMC absorber, the 2-d distributions of the incident electric field (amplitude and phase) were consistently measured. In addition to the RF power distribution measurement [4], the amplitude and phase information should be quite useful in identifying the direction-of-arrivals and source locations of the incoming waves. Thus this technique could be applied to localizing RF noise sources in electronic equipment under actual operating conditions, as well as to evaluating the performance of antennas mounted on wireless communication devices used in real environments.

It is necessary to further evaluate the accuracy of this technique, by investigating the effects of the edge reflection from the finite-sized absorber, of the oblique incidence, and of the additional lumped elements such as varactors to control the resonance (absorption) frequency [4][6]. Practical validation of this technique by fabricating an AMC absorber with an array of RF voltage detectors is being performed by the authors and will be reported soon.

Acknowledgment

The authors would like to thank Dr. M. Ozaki of Kanazawa University for his valuable suggestions and discussions.

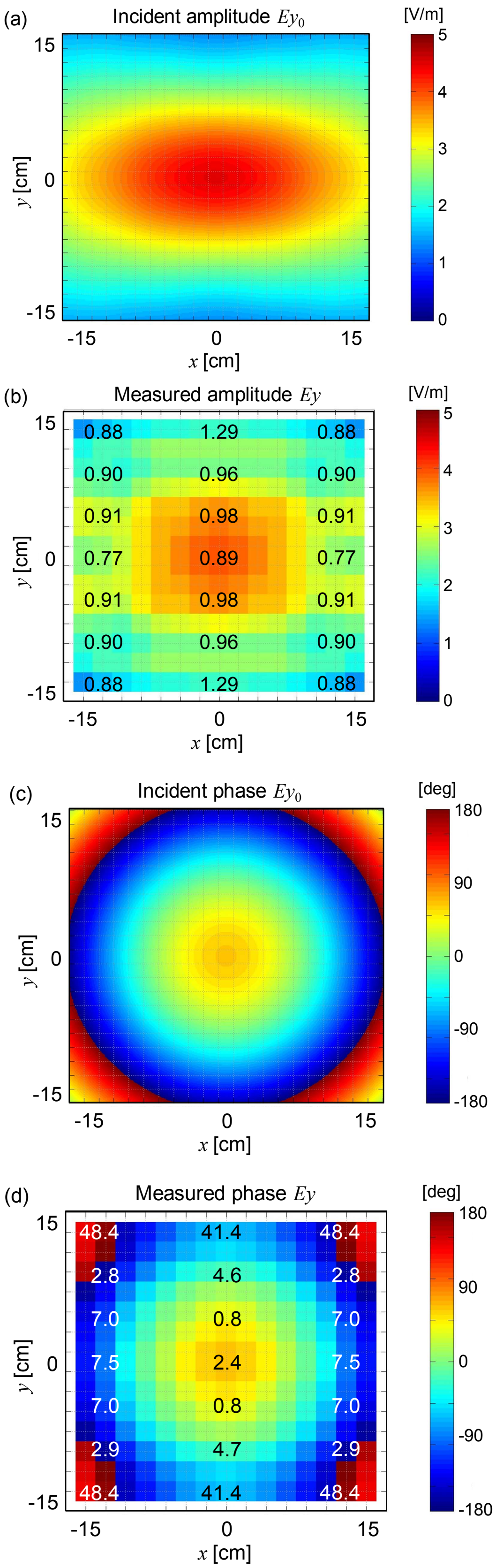

Fig. 4. Two-dimensional distributions of (a) incident electric field amplitude, (b) measured electric field amplitude, (c) incident phase and (d) measured phase for a spherical-wave illuminating the absorber surface

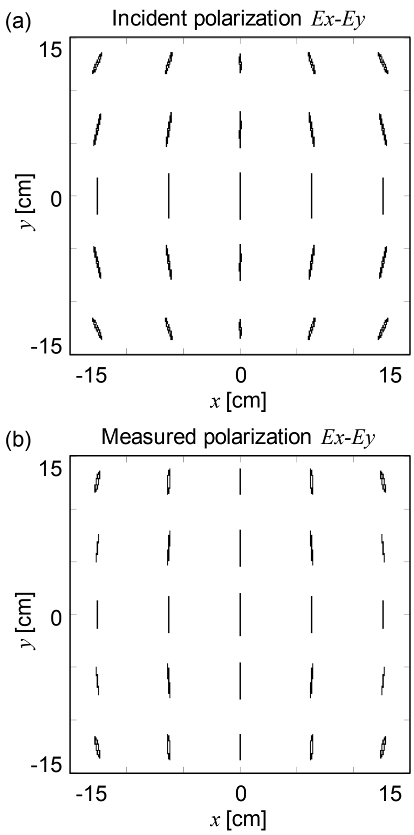

Fig. 5. Two-dimensional distributions of electric field vectors (polarizations) of the spherical-wave on the absorber surface: (a) incident electric field vectors and (b) measured electric field vectors

REFERENCES

[1] N. Engheta and R. W. Ziolkowski Ed., *Metamaterials*, Wiley-IEEE Press, 2006.

[2] Y. Kotsuka, K. Murano, M. Amano, and S. Sugiyama, "Novel right-handed metamaterial based on the concept of "Autonomous Control System of Living Cells" and its absorber applications," *IEEE Trans. Electromagnetic Compatibility*, vol. 52, no.3, pp. 556–565, Aug. 2010.

[3] O. Luukkonen, F. Costa, C. R. Simovski, A. Monorchio, and S. A. Tretyakov, "A thin electromagnetic absorber for wide incidence angles and both polarizations," *IEEE Trans. Antennas and Propagation*, vol. 57, no. 10, pp. 3119–3125, Oct. 2009.

[4] S. Yagitani, K. Katsuda, M. Nojima, Y. Yoshimura, and H. Sugiura, "Imaging radio-frequency power distributions by an EBG absorber," IEICE Trans. Commun., vol. E94-B, no. 8, pp.2306–2315, Aug. 2011.

[5] D. Sievenpiper, L. Zhang, R. F. J. Broas, N. G. Alexopolous, and E. Yablonovitch, "High-impedance electromagnetic surfaces with a forbidden frequency band," IEEE Trans. Microwave Theory Tech., vol. 47, no. 11, pp. 2059–2074, Nov. 1999.

[6] S. Yagitani, K. Katsuda, R. Tanaka, M. Nojima, Y. Yoshimura, and H. Sugiura, "A tunable EBG absorber for radio-frequency power imaging," Proc. 30th URSI General Assembly and Scientific Symposium, 4 pages, Aug. 2011.